

Vibrational Spectroscopy

Elixir Vib. Spec. 92 (2016) 39112-39120

Elixir
ISSN: 2229-712X

Spectroscopic investigation (FT-IR and FT-Raman), vibrational assignments, HOMO-LUMO, NBO and MESP analyses of 3'-Nitroacetophenone

S. Manivel¹, M. Arivazhagan^{1*}, E. Palanisamy² and R. John James

¹ PG and Research Department of Physics, Govt. Arts College, Trichy-22, Tamil Nadu, India.

² PG and Research Department of Physics, Govt. Arts College, Karur -5 Tamil Nadu, India.

ARTICLE INFO

Article history:

Received: 4 March 2016;

Received in revised form:

12 March 2016;

Accepted: 17 March 2016;

Keywords

3'-Nitroacetophenone,
DFT,
ab initio,
NBO,
NLO,
MESP.

ABSTRACT

In this work, the experimental and theoretical vibrational spectra of 3'-nitroacetophenone [3'NAP] were studied. FTIR and FT Raman spectra were recorded in the region 4000–400 cm⁻¹ and 4000–50 cm⁻¹, respectively. The structural and spectroscopic data of the molecule in the ground state were calculated by using ab initio Hartree–Fock and density functional method (B3LYP) with the 6-311++G(d,p) basis set. The vibrational frequencies were calculated and scaled values were compared with experimental FTIR and FT Raman spectra. The observed and calculated frequencies are found to be in good agreement. The complete assignments were performed on the basis of the total energy distribution (TED) of the vibrational modes, calculated with scaled quantum mechanics (SQM) method. The optimized geometric parameters were calculated. The predicted first hyperpolarizability also shows that the molecule might have a reasonably good nonlinear optical (NLO) behaviour. The calculated HOMO–LUMO energy gap reveals that the charge transfer occurs within the molecule besides, molecular electrostatic potential (MEP),

© 2016 Elixir All rights reserved.

Introduction

Acetophenone is one of the most aromatic carbonyl, which shows interesting photochemical properties [1, 2]. Acetophenone are compound that exhibit interesting physicochemical and biological properties. They are found in nature [3, 4] and they can also be obtained by means of diverse synthesis procedures [5, 6]. Antibacterial activity can be mentioned among its biological properties. A recent study has linked the antibacterial activity of 20 acetophenone with their structural characteristics by using electronic and topological indices [7]. On the other hand, substituted acetophenone are employed as synthesis reagents of several organic reactions. A well known one is the condensation reaction in alkaline medium of acetophenones and benzaldehydes in the synthesis of flavonoids (chalcones, flavones and flavanones) [8, 9].

However, the detailed HF and B3LYP/6-311++G(d,p) comparative studies on the complete FT-IR and FT-Raman spectra of 3'-nitro acetophenone [3'NAP] have not been reported so far. In view of these special properties and uses, the present investigation has been undertaken to provide a satisfactorily vibrational analysis of 3'-nitroacetophenone[3'NAP]. Therefore, a thorough Raman, IR, molecular electrostatic potential [MESP], non-linear optical (NLO) Properties, HOMO-LUMO, NBO, UV and error analyses are reported complemented by B3LYP theoretical predictions with basis sets 6-311++G(d,p) to provide novel on vibrational assignments and conformational stability of [3'NAP]

Experimental Details

The pure sample of 3'NAP in the light yellow liquid form was purchased from the Lancaster Chemical Company (UK), with a stated purity of greater than 98% and it was used as such without further purification. The FT-IR spectrum of this compound was recorded in the region 4000–400 cm⁻¹ on BRUKER IFS 66V spectrometer equipped with an MCT detector using KBr beam splitter and global arc source. The FT-Raman spectrum of title molecule has been recorded using the 1064 nm line of a Nd:YAG laser as excitation wavelength in the region 4000–50 cm⁻¹ on a BRUKER model RFS 66V spectrometer. The reported wavenumbers are expected to be accurate within ±1 cm⁻¹ resolution with 250 mW of power at the sample in both the techniques.

Computational Details

The molecular structure of 3'NAP in the ground state is computed using HF and B3LYP with 6-311++G (d,p) and 6-311++G(d,p) basis set. All the computations have been done by adding polarization function and diffuse function on heavy atoms[10-11], in addition to triple split valence basis set 6-311++G(d,p), for better treatment of polar bond of methyl group. The calculated frequencies are scaled by 0.890, and 0.852 for HF and for B3LYP with 6-311++G(d,p) basis set by 0.934, 0.940, 0.982, 0.952, 0.889 and 0.969 [12]. The theoretical result have enabled us to make the detailed assignments of the experimental IR and Raman of the title compound. The DFT and HF calculations for 3'NAP are performed using GAUSSIAN 09W Program without any constraint on the geometry [13].

By combining the result of the MOLVIB program (version V7.0-G77) [14-16] with symmetry considerations, vibrational frequency assignments were made with a high degree of accuracy. However, the defined coordinates forms complete set and matches quite well with the motions observed using GAUSSVIEW program.

Prediction of Raman Intensities

The Raman activities are subsequently converted to relative Raman intensities (I_i) using the following relationship derived from the basic theory of Raman scattering [17-19]:

$$I_i = \frac{f(\nu_o - \nu_i)^4 S_i}{n_i \left[1 - \exp\left(-\frac{hc\nu_i}{kT}\right) \right]} \quad (1)$$

where, ν_o is the laser exciting wave number in cm^{-1} (in this, the used excitation wave number $\nu_o = 9398.5 \text{ cm}^{-1}$, which corresponds to the wavelength of 1064 nm of a Nd:YAG laser), ν_i is the vibrational wave number of the i^{th} normal mode (cm^{-1}), while S_i is the Raman scattering activity of the normal mode ν_i , f (is a constant equal to 10^{-12}) is a suitably chosen common normalization factor for all peak intensities. h , k , c and T are Planck and Boltzmann constants, speed of light and temperature in Kelvin, respectively.

Results and discussions

The labelling of atoms of the 3'NAP is shown in Fig.1. The zero point vibrational energy of the 3'NAP at HF/6-311++G(d,p) and B3LYP/6-311++G(d,p) levels are -585.63575 a.u kcal/mol and -589.34679 a.u kcal/mol. The comparative optimized structural parameters such as bond lengths, bond angles and dihedral of 3'NAP are presented in Table 1 from the theoretical values, it is found that most of the optimized bond lengths are slightly larger than the experimental values, due to that the theoretical calculations belonging to isolated molecules in gaseous phase while experimental. Results belong to molecules in solid state [20].

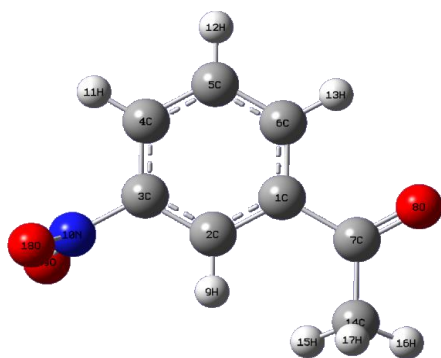


Fig 1. Molecular structure of 3'-nitroacetophenone.

The phenyl ring appears little distorted and angles slightly out of perfect hexagonal structure. It is due to the substitutions of the carbon atoms. oxygen atoms in the place of H atoms. According to the experimental value [21] order of the optimized lengths of the six C-C bonds of the ring are as $C5-C6 < C2-C3 < C1-C2 < C1-C6 < C4-C5 < C3-C4$ According to the calculated values for the compounds at HF/B3LYP/6-311++G(d,p) and 6-311++G(d,p) the order of the bond lengths is slightly differed as $C2-C3 < C4-C5 < C1-C6 < C5-C6 < C3-C4 < C1-C2$ in 3'NAP The benzene ring appears to be distorted with C1-C2 and C1-C6 bond lengths exactly at the substitution place [22-24].

Vibrational spectra

The 3'NAP consist of 19 atom, hence under goes 51 normal modes of vibrations in agreement with C_s symmetry species

$$|3N - 6 = 35A' \text{ (in plane)} + 16A'' \text{ (out-of-plane)}$$

all the 51 fundamental vibrations are active in both Raman scattering and IR absorption. The harmonic vibrational frequencies are calculated at HF and B3LYP levels using 6-311++G(d,p) and 6-311++G(d,p) basis set along with the diffuse and polarization function of vibrations have been presented in Table 2. The FTIR and FT-Raman spectrum of 3'NAP are shown in Figs 2 and 3.

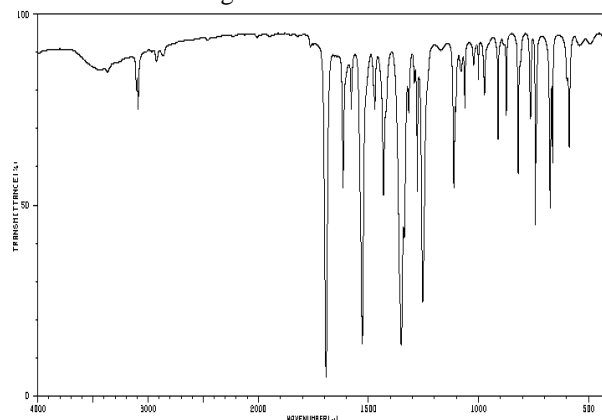


Fig 2. FTIR spectrum of 3'- nitroacetophenone.

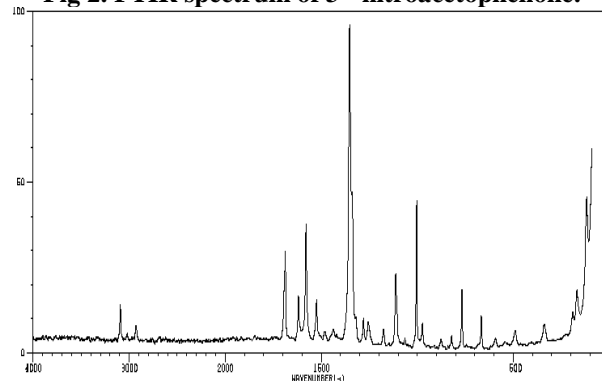


Fig 3. FT-Raman spectrum of 3'- nitroacetophenone.

C-H vibrations

Aromatic compounds commonly exhibit multiple weak bands in the region $3100-3000 \text{ cm}^{-1}$ due to aromatic C-H stretching vibrations [25]. Hence, the infrared bands appeared at 3107, 3098 cm^{-1} and the Raman bands found at 3010, 2950 cm^{-1} in 3'NAP have been assigned to C-H stretching vibrations and these modes are confirmed by their TED values. The bands due to C-H in-plane bending vibrations, interact somewhat with C-C stretching vibrations, are observed as a number of sharp bands in the region $1300-1000 \text{ cm}^{-1}$ The C-H out-of-plane bending vibrations are strongly coupled vibrations and occur in the region $900-667 \text{ cm}^{-1}$. The FT-Raman bands observed at 1240, 1190 cm^{-1} and infrared bands at 1254 cm^{-1} are assigned to C-H in-plane bending vibrations of 3'NAP. The out-of plane bending vibrations of C-H group have also been identified for 3'NAP and they are presented in Table 2.

C=O vibrations

The carbonyl group vibrational frequencies are the significant characteristic bands in the vibrational spectra of ketones, and for this reason, such bands have been the subject of extensive studies [26].

Table 1. Optimized geometrical parameters of 3'- nitroacetophenone obtained by HF/6-311++G(d,p) and B3LYP/ 6-311++G(d,p) methods and basis set.

Bond Length	Value (Å)		Experimental ^a	Bond Angle	Value (°)		Experimental ^a	Dihedral Angle	Value (°)	
	6-311++G(d,p)/ 6-311++G(d,p)				6-311++G(d,p)/ 6-311++G(d,p)				6-311++G(d,p) / 6-311++G(d,p)	
	HF	B3LYP			HF	B3LYP			HF	B3LYP
C1-C2	1.3877	1.3999	1.390	C2-C1-C6	119.2409	119.2523	116.7	C6-C1-C2-C3	0.0027	-0.0012
C1-C6	1.396	1.4074	1.396	C2-C1-C7	121.9038	121.9598	119.7	C6-C1-C2-H9	-179.9983	179.9977
C1-C7	1.4932	1.4979	1.468	C6-C1-C7	118.8553	118.7879	123.6	C7-C1-C2-C3	-179.9983	-179.9985
C2-C3	1.3851	1.3942	1.370	C1-C2-C3	119.0731	119.0364	122.3	C7-C1-C2-H9	-0.0002	0.0004
C2-H9	1.069	1.0784	-	C1-C2-H9	121.9394	122.1436	-	C2-C1-C6-C5	-0.0008	0.0009
C3-C4	1.3844	1.3949	1.399	C3-C2-H9	118.6907	118.82	-	C2-C1-C6-H13	179.9992	-179.9989
C3-N10	1.4495	1.4664	-	C2-C3-C4	122.2345	122.2278	120.3	C7-C1-C6-C5	180.0001	179.9982
C4-C5	1.3861	1.3964	1.398	C2-C3-N10	118.6907	118.7248	-	C7-C1-C6-H13	0.0001	-0.0016
C4-H11	1.0701	1.0789	-	C4-C3-N10	119.0748	119.0474	-	C2-C1-C7-O8	-179.9944	+179.9871
C5-C6	1.3861	1.3945	1.369	C3-C4-C5	118.504	118.4656	120.5	C2-C1-C7-C14	0.0063	-0.0141
C5-H12	1.0715	1.0808	-	C3-C4-H11	120.0491	119.7272	-	C6-C1-C7-O8	0.0047	-0.0102
C6-H13	1.0716	1.0807	-	C5-C4-H11	121.4469	121.8073	120.5	C2-C1-C7-C14	-179.9997	179.9887
C7-O8	1.222	1.2452	1.215	C4-C5-C6	120.0986	120.2745	-	C1-C2-C3-C4	-0.0035	0.0012
C7-C14	1.5034	1.5084	1.495	C4-C5-H12	119.7279	119.6159	122.1	C1-C2-C3-N10	-180.0016	-179.9982
N10-O18	1.2272	1.2672	-	C6-C5-H12	120.1734	120.1097	-	H9-C2-C3-C4	179.9984	-179.9977
N10-O19	1.2293	1.2685	-	C1-C6-C5	120.8489	120.7434	-	H9-C2-C3-N10	0.0003	0.0029
C14-H16	1.0841	1.0928	1.090	C1-C6-H13	118.5234	118.1443	-	C2-C3-C4-C5	0.0023	-0.0009
C14-H16	1.079	1.0866	1.090	C5-C6-H13	120.6277	121.119	-	C2-C3-C4-H11	-179.9982	-180.0011
C14-H17	1.0841	1.0928	1.090	C1-C7-O8	119.5532	119.6482	120.1	N10-C3-C4-C5	180.004	-180.0015
				C1-C7-C14	119.8794	119.7036	-	N10-C3-C4-H11	-0.001	-0.0017
				O8-C7-C14	120.5673	120.6482	-	C2-C3-N10-O18	179.9898	179.9993
				C3-N10-O18	118.3165	118.2715	-	C2-C3-N10-O19	-0.0001	-0.0015
				C3-N10-O19	123.3909	118.2686	-	C2-C3-N10-O18	-0.0083	-0.0002
				O18-N10-O19	123.3909	123.4599	-	C4-C3-N10-O19	179.9824	179.9991
				C7-C14-H15	111.1917	111.3648	-	C3-C4-C5-C6	-0.0003	0.0005
				C7-C14-H16	108.5313	108.7524	-	C3-C4-C5-H12	179.9993	180.0005
				C7-C14-H17	111.1922	111.3657	-	H11-C4-C5-C6	180.002	180.007
				H15-C14-H16	108.9557	108.9292	-	H11-C4-C5-H12	-0.0002	0.0007
				H15-C14-H17	107.9696	107.442	-	C4-C5-C6-C1	-0.004	-0.0006
				H16-C14-H17	108.9532	108.9293	-	C4-C5-C6-H13	179.9996	179.9993
								H12-C5-C6-C1	180.0	179.9994
								H12-C5-C6-H13	0.0	-0.0007
								C1-C7-C14-H15	60.1833	59.9778
								C1-C7-C14-H16	180.0121	180.0223
								C1-C7-C14-H17	-60.1619	-59.9325
								O8-C7-C14-H15	-119.8161	-120.0234
								O8-C7-C14-H16	0.0127	0.0211
								O8-C7-C14-H17	119.8387	120.0663

For numbering of atoms refer Fig.1

^aExperimental values are taken from Ref [22].

The intensity of these bands can increase because of conjugation, therefore, leads to the intensification of the Raman lines as well as the increased infrared band intensities. The carbonyl stretching vibrations in ketones are expected in the region 1680–1715 cm⁻¹. In this case, the band observed at 1318 cm⁻¹ IR spectra is assigned as C=O stretching vibration. The vibrational bands observed at

650 and 490 cm⁻¹ in Raman are assigned to C=O in-plane and out-of-plane bending vibrations for 3'NAP, respectively. These vibrational assignments are in line with the literature [27]

C-C vibrations

The C-C aromatic stretching vibrations gives rise to characteristic bands in both the observed IR and Raman spectra [28], covering the spectral range from 1600 to 1400 cm⁻¹. Therefore, the C-C stretching vibrations of 3'NAP are found at, 1616,1529,1471,1432 and 1338 cm⁻¹ in FTIR and 1685,1610,1490,1470, and 1350,cm⁻¹ in the FT-Raman

spectrum and these modes are confirmed by their TED values. Most of the ring vibrational modes are affected by the substitutions in the aromatic ring of 3'NAP. In the present study, the bands observed at 1104 cm⁻¹ and 1150,1110,1060 cm⁻¹ in the FTIR and Raman spectrum, respectively, have been designated to ring in-plane bending modes by carefully consideration of their quantitative descriptions. The ring out-of-plane bending modes of 3'NAP are also listed in the Table 2. The reductions in the frequencies of these modes are due to the change in force constant and the vibrations of the functional groups present in the molecule.

CH₃ group vibrations

The 3'NAP possess only one CH₃ group in the ring. The methyl group stretching vibrations are highly localized and generally observed in the range 3000–2900 cm⁻¹ [29–30].

In the present investigation, the bands with sharp peaks are found at 2925, 2862 cm⁻¹ in IR and 2910 cm⁻¹ in Raman for the CH₃ stretching vibrations of methyl group.

Table 2. The observed (FT-IR and FT-Raman) and calculated (Unscaled and Scaled) frequencies (cm^{-1}), IR intensities (Km mol^{-1}), Raman intensities ($\text{\AA}^4 \text{amu}^{-1}$), force constant and probable assignments (characterized by TED) of 3'- nitroacetophenone using HF and B3LYP/6-311++G(d,p) and 6-311++G(d,p) calculations.

S. N o.	Observed frequencies (cm^{-1})			Calculated values									Vibrational assignments (% TED)	
	Symmetry species C_s	FT-IR	FT-Raman	HF/6-311++G(d,p)					B3LYP/6-311++G(d,p)					
				Frequencies (cm^{-1})		IR intensity	Raman intensity	Force constant	Frequencies (cm^{-1})		IR intensity	Raman intensity		Force constant
				Unscaled	Scaled				Unscaled	Scaled				
1.	A'	3107		3429	3115	5.0248	34.8376	7.5910	3311	3104	7.0117	22.3699	7.1045	γ CH(98)
2.	A'	3098		3427	3105	1.8663	52.2310	7.5926	3309	3097	4.2464	89.7056	7.0791	γ CH(98)
3.	A'		3010	3421	3017	3.4073	34.1256	7.6035	3307	3007	6.1095	18.3420	7.0795	γ CH(98)
4.	A'		2950	3417	2958	0.5588	33.1872	7.5254	3299	2947	0.0291	25.6588	7.0014	γ CH(97)
5.	A'	2925		3407	2930	6.4676	113.5817	7.5204	3295	2920	3.1329	107.585	7.0052	γ CH ₃ ips (98)
6.	A'		2910	3401	2915	1.8842	23.6013	7.4342	3285	2906	1.8944	22.2119	6.9214	γ CH ₃ ss(98)
7.	A'	2862		3319	2868	4.2547	62.3849	6.7012	3207	2798	2.5776	71.1041	6.2535	γ CH ₃ ops(80)
8.	A'	1693		1763	1699	3.5476	20.8498	8.5778	1634	1688	9.2607	2.7126	10.5738	NO ₂ ass (88)
9.	A'		1685	1752	1689	2.9542	10.3063	9.6405	1625	1680	0.5730	27.8643	8.8384	γ CC (80) CH (20)
10	A'	1616	1610	1663	1620	179.6632	22.9665	4.7881	1564	1609	148.5837	48.7609	7.5854	γ CC (80) CO(10)CH(10)
11	A'	-	1590	1645	1595	22.6772	12.1764	2.1727	1518	1583	9.7471	5.4988	1.9281	γ CH ₃ ipb (96)
12	A'	1578	-	1629	1583	4.5606	2.0941	2.4258	1502	1570	6.9143	2.7490	1.8949	γ CH ₃ Sb(96)
13	A'	-	1540	1595	1547	52.2933	28.9076	1.8634	1470	1533	25.9194	51.3574	1.5024	CH ₃ opb(96)
14	A'	1529	-	1557	1533	49.1968	13.9558	4.0344	1455	1523	22.4290	49.1653	3.2651	γ CC (80) CH ₃ (17)
15	A'	-	1490	1528	1496	21.7985	2.6545	1.6220	1378	1436	34.2704	75.3759	1.3241	γ CC (84) C-H(15)
16	A'	1471	1470	1476	1478	0.8914	1.2906	1.6465	1351	1466	2.8503	6.3397	3.0019	γ CC (80)
17	A'	1432	-	1341	1436	45.8110	14.1504	2.1484	1341	1427	6.9230	1.8356	2.0096	γ CC (80) CN(15)
18	A'	1362	-	1318	1367	93.5256	109.658	3.1974	1227	1358	79.1652	235.1695	4.8864	NO ₂ ss(88)
19	A'	-	1350	1282	1357	45.9542	12.6625	2.3282	1203	1346	8.7358	36.3036	0.9863	γ CC (80) CN(18)
20	A'	1338	-	1254	1443	8.9737	44.1695	3.0919	1178	1331	142.7659	58.8977	2.1071	γ CC (80)
21	A'	1318	-	1201	1324	0.0618	0.5621	1.3384	1113	1315	6.2070	3.4308	1.1544	γ C O(78)
22	A'	1292	-	1200	1298	0.3919	1.1663	1.4110	1087	1387	14.5372	30.5829	1.513	γ CN (92)
23	A'	1278	1280	1181	1283	12.7516	26.3536	1.7417	1043	1272	1.3269	2.8893	1.2959	bCH (78) CN(12)
24	A'	1254	-	1167	1259	2.1583	4.7392	1.4876	1035	1249	8.6590	136.2856	3.7616	bCH(76) CC (18)
25	A'	-	1240	1122	1248	1.1929	0.8574	1.0583	1017	1237	32.8394	33.0850	4.1207	bCH(78)
26	A'	-	1190	1105	1196	6.0184	152.9884	4.2216	1002	1185	0.2176	0.0732	0.8392	bCH(78)
27	A'	-	1150	1086	1158	6.1902	0.3443	1.0581	982	1145	135.1740	34.7549	4.4074	Rtrigd(94)
28	A'	-	1140	1059	1149	22.4603	24.0673	3.1844	942	1137	12.1019	6.3839	0.8108	CH ₃ ipr(68)
29	A'	1104	1110	1019	1116	25.4007	12.6039	1.9062	936	1097	29.7584	18.9535	1.2569	Rsymd(68)
30	A'	1063	1060	941	1067	9.7649	0.6614	0.7725	903	1056	37.4501	5.6926	0.7501	Rasymd(68)
31	A'	1023	-	844	1028	10.4472	8.1011	4.1883	795	1019	11.7971	10.1068	1.9913	bCC (75)
32	A'	1001	1002	803	1008	156.5869	3.3704	1.2811	792	997	48.6303	7.6673	0.6353	bCC(75) CN(15)
33	A'	-	990	796	997	60.1542	9.9109	2.3281	737	980	1.9725	10.2466	3.1785	t Rtrigd(44) CN(20) CC(20)
34	A'	973	-	765	978	9.5426	0.5876	0.7819	693	960	0.3677	68.9289	2.1594	t Rasymd(44)
35	A'	912	-	731	919	5.4488	52.2345	2.2040	672	903	30.9376	0.1218	0.5046	t Rasymd(44) CC(16)
36	A''	880	874	650	888	68.6848	16.8675	0.8116	655	870	12.1463	38.1409	2.7126	CH ₃ opr(56)
37	A''	820	821	646	826	7.4411	89.8914	3.4651	638	810	1.7304	0.19506	0.8733	ω CH(55) CO(15)
38	A''	-	770	619	776	34.1980	19.6054	0.9403	573	760	24.4008	16.6106	0.8114	NO ₂ sciss(61) CH(18)
39	A''	755	-	507	759	5.1718	2.0695	0.6970	528	745	2.4163	10.4004	0.5425	ω CH(55) C-C(17)
40	A''	742	-	496	747	6.2759	2.4789	0.5208	464	732	2.2000	1.7347	0.5586	ω CH(55)
41	A''	676	-	460	680	23.5843	13.3337	0.4943	415	666	0.1187	4.5221	0.3211	NO ₂ rock(60)
42	A''	664	-	395	668	0.5737	11.8851	0.3737	367	654	1.0468	9.8793	0.3433	ω CH(55)
43	A''	-	650	361	656	10.4650	42.8677	0.6250	361	640	0.8988	11.3714	0.3606	bC-O(54)
44	A''	599	-	326	603	0.8328	22.8760	0.3953	338	589	6.2936	35.022	0.5880	bC-N(60)
45	A''	-	590	250	596	0.0648	38.7008	0.2783	286	580	0.6586	14.0121	0.2790	ω CC(52)
46	A''	550	-	247	557	0.0661	26.7835	0.2269	195	540	0.3263	32.1378	0.1152	ω CC(52)
47	A''	-	490	197	496	4.3556	14.8177	0.1527	190	480	0.2620	20.6686	0.2032	ω CO(48)
48	A''	480	-	191	487	8.7964	6.2562	0.1279	166	465	8.7840	5.8086	0.0936	ω CN(40)
49	A''	-	350	102	356	8.9711	8.0320	0.0208	136	339	3.3401	21.9277	0.0710	NO ₂ twisting(61)
50	A''	-	165	-261	169	422.8857	1.4047	0.5977	-32	155	5.9366	8.8161	0.0019	NO ₂ wagging(61)
51	A''	-	115	-112	119	0.0800	5.6058	0.0591	-403	105	0.0831	10.3057	0.0973	τ CH ₃ (38)

Abbreviations: v – stretching; ss – symmetric stretching; ass – asymmetric stretching; b – bending; ω – out-of-plane bending; R – ring; trigd – trigonal deformation; symd – symmetric deformation; asymd – antisymmetric deformation; t – torsion; s – strong; vs – very strong; ms – medium strong; w – weak; vw – very weak

These observations agree well with the earlier work [31-32]. The CH₃ in-plane bending vibration is observed at 1590 cm⁻¹ in Raman. The symmetrical methyl deformation mode (CH₃sb) is established at 1578 cm⁻¹ in the IR spectrum for 3'NAP. The CH₃ out-of-plane bending vibration is found at 1540 cm⁻¹. These frequencies are in good agreement with those found in the characteristic group frequency table 2 [33-34]. The theoretically computed value by B3LYP6-311++G (d,p) method for CH₃ in-plane bending is nearly coincides with the experimental value. The bands obtained at 880, 1140 cm⁻¹ and 874 cm⁻¹ in IR and Raman spectra are assigned to CH₃ in-plane and out-of-plane rocking modes, respectively, and they show good agreement with the calculated values.

NO₂ vibrations

The characteristic group frequencies of the nitro group are relatively independent of the rest of the molecule which makes this group convenient to identify. Aromatic nitro compounds have strong absorptions due to the asymmetric and symmetric stretching vibrations of the NO₂ group at 1570–1485cm⁻¹ and 1370–1320cm⁻¹, respectively [35]. Hence, the asymmetric stretching mode of nitro group for 3'NAP is identified at 1693cm⁻¹ in FTIR, spectrum and in good agreement with TED output. The symmetric stretching mode of nitro group is assigned at 1362cm⁻¹ in IR spectrum. The NO₂ scissoring mode has been designated to the band at 770 cm⁻¹ in Raman spectrum, respectively. The deformation vibrations of NO₂ group (rocking, wagging and twisting) contribute to several normal modes in the low frequency region [36]. These bands were also found well within the characteristic region and summarized in Table 2

NBO analysis

NBO analysis is proved to be an effective tool for chemical interpretation of hyper conjugative interaction and electron density transfer (EDT) from filled lone electron pairs of the n (Y) of the "Lewis base" Y into the unfilled antibond σ^* (X-H) of the "Lewis acid" X-H in X-H...Y hydrogen bonding systems [37]. Also, in order to obtain structure of molecule 3'NAP, the main natural orbital interactions were analyzed with the NBO 3.1 program [38]. The lowering of orbital energy due to the interaction between the doubly occupied orbital and the unoccupied ones is a very convenient guide to interpret the molecular structure. In energetic terms, hyperconjugation is an important effect [39-40] in which an occupied Lewis-type natural bond orbitals stabilized by overlapping with a non Lewis-type orbital (either one-center

Rydberg's or two-center antibonding NBO). This electron delocalization can be described as a charge transfer from a Lewis valence orbital (donor), with a decreasing of its occupancy, to a non-Lewis orbital (acceptor). Several other types of valence data, such as directionality, hybridization and partial charges, were analyzed in the output of NBO analysis Table 3 and 4 gives the second-order perturbation energy, Eij(2) corresponding to the interactions and the overlap integral of each orbital pair. From the table very strong hyper conjugative interaction is observed between the π type orbital containing the lone electron pair of O₁₈ and the neighbor (C3-N10) anti-bonding orbital of the benzene ring. This interaction is responsible for a pronounced of the lone pair orbital occupancy. The hyper conjugation between O₁₈ and the benzene ring defines the common molecular feature of this type of molecules. An important contribution for the molecular stabilization energy is further given by O18 through the overlap of its sp^{0.25} lone pair (LP (1) O18) with the π^* (C3-N10) orbital and shows the hyper conjugation interaction.

Molecular Electrostatic Potential

Molecular electrostatic potential (MESP) at a point in the space around a molecule gives an indication of the net electrostatic effect produced at that point by the total charge distribution (electron + nuclei) of the molecule and correlates with dipole moments, electro negativity, partial charges, and chemical reactivity of the molecule. It provides a visual method to understand the relative polarity of the molecule. An electron density isosurface mapped with electrostatic potential surface depicts the size, shape, charge density, and site of chemical reactivity of the molecule. Different values of the electrostatic potential are represented by different colors: red represents the regions of the most negative electrostatic potential, blue represents the regions of the most positive electrostatic potential, and green represents the region of zero potential. Potential increases in the following order: red < orange < yellow < green < blue. Such mapped electrostatic potential surfaces have been plotted for the title molecule by B3LYP/6-311++G(d,p) method using the computer software Gaussian 09 package. In the present study, 3D plots of molecular electrostatic potential (MEP) of 3'-Nitroacetophenone is illustrated in Fig 4.

The color code of MEP is in the range between -5.706 a.u. (red) to 5.706 a.u. (blue) in the title compound, where blue indicates the strongest attraction and red indicates the strongest repulsion.

Table 3. NBO results showing the formation of Lewis and non Lewis orbitals by valence hybrids corresponding to the inter molecule of 3'- nitroacetophenone using B3LYP/6-311+G(d,p) level calculation.

Bond A-B	Occupancy	ED _A	ED _B	NBO%	S%	P%
BD(C1-C2)	1.97257	50.30	49.70	0.7092 ^{SP1.89} + 0.7050 ^{SP1.78}	34.63, 35.97	65.37, 64.03
BD*(C1-C2)	0.02213	49.70	50.30	0.7050 ^{SP1.89} + 0.7092 ^{SP1.78}	34.63, 35.97	65.37, 64.03
BD(C3-N10)	1.98931	36.63	63.37	0.6053 ^{SP3.24} + 0.7960 ^{SP1.66}	23.60, 37.62	76.40, 68.38
BD*(C3-N10)	0.09270	63.37	36.63	0.7960 ^{SP3.24} + -0.6053 ^{SP1.66}	23.60, 37.62	76.40, 68.38
BD(C7-O8)	1.99481	35.20	64.80	0.5933 ^{SP2.33} + 0.8050 ^{SP1.65}	30.02, 37.70	69.98, 62.30
BD*(C7-O8)	0.01215	64.80	35.20	0.8050 ^{SP2.33} + 0.5933 ^{SP1.65}	30.02, 37.70	69.98, 62.30
BD(N10-O18)	1.99519	50.57	49.43	0.7111 ^{SP2.22} + 0.7031 ^{SP4.04}	31.10, 19.84	68.90, 80.16
BD*(N10-O18)	0.05508	49.43	50.57	0.7031 ^{SP2.22} + -0.7111 ^{SP4.04}	31.10, 19.84	68.90, 80.16
BD(N10-O19)	1.99522	50.58	49.42	0.7112 ^{SP2.22} + 0.7030 ^{SP4.05}	31.07, 19.78	68.93, 80.22
BD*(N10-O19)	0.05588	49.42	50.58	0.7030 ^{SP2.22} + -0.7112 ^{SP4.05}	31.07, 19.78	68.93, 80.22
LP(1) O8	1.97862	-	-	SP ^{0.61}	62.30	37.70
LP(1) O18	1.98271	-	-	SP ^{0.25}	79.94	20.06
LP(O19)	1.98274	-	-	SP ^{0.25}	79.97	20.03

The negative (red) regions of MEP were related to electrophilic reactivity and the positive (blue) regions to nucleophilic reactivity are shown in Fig. 4. As can be seen from the figure and the calculated results, this molecule has several possible sites for electrophilic attack over oxygen atom. For possible nucleophilic reactions the maximum positive region is found on the hydrogen atoms of the benzene ring.

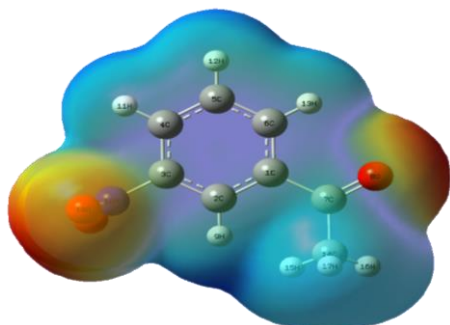


Fig 4. Molecular electrostatic potential map (MEP) for 3'-nitroacetophenone.

Table 4: Second order perturbation energies (E^2) kcal (mol) corresponding of the most importance charge transfer interaction (donor – acceptor) in the compounds studied by B3LYP 6-311++G(d,p).

S.No	Bond	Acceptor	E^2	$E(j-E_i)$	$F(i,j)$
1.	BD(C1-C2)	BD*C3-N10	4.08	0.98	0.057
2.	BD(C3-N10)	BD*C1-C2	1.50	1.37	0.041
3.	BD(C7-O8)	BD*C1-C2	1.50	1.59	0.44
4.	BD(N10-O18)	BD*C3-N10	0.56	1.30	0.025
5.	BD(N10-O19)	BD*C3-C4	0.88	1.56	0.033
6.	LP(1) O8	RY*C7	14.67	1.59	0.137
7.	LP(1) O18	BD*C3-N10	4.30	1.08	0.062
8.	LP(O19)	N10	5.34	1.88	0.089

Non-Linear Optical (Nlo) Properties

The quantum chemistry based prediction of non-linear optical (NLO) properties of a molecule has an important role for the bonding and delocalization of electron density from occupied Lewis-type (donor) NBOs to properly unoccupied non-Lewis type design of materials in modern communication technology, signal processing and optical interconnections [41]. Especially organic molecules are studied because of their larger NLO susceptibilities arising from π -electron cloud movement from donor to acceptor, fast NLO response times, high laser damage thresholds and low dielectric constants. Although the organic molecules have these advantages, they have several NLO disadvantages too they have generally low thermal stability and they may undergo a facile relaxation to random orientation [42]. In addition, in the UV–VIS region, the low energy transitions result in a trade-off between the nonlinear efficiency and optical transparency [43–44]. But the usage of organic molecules as ligand can overcome these disadvantages. The tensor components of the static first hyperpolarizability (β) were analytically calculated by using the same method as mentioned above. From the computed tensorial components, β is calculated for the title molecule by taking into account the Kleinman symmetry relations and the square norm of the Cartesian expression for the β tensor [45]. The relevant expressions used for the calculation are shown below.

$$\beta = (\beta_x^2 + \beta_y^2 + \beta_z^2)^{1/2}$$

where

$$\beta_x = \beta_{xxx} + \beta_{xyy} + \beta_{xzz}$$

$$\beta_y = \beta_{yyy} + \beta_{xxy} + \beta_{yzz}$$

$$\beta_z = \beta_{zzz} + \beta_{xxz} + \beta_{yyz}$$

The components of dipole moment, the first hyperpolarizability of the title compound can be seen in Table 5. The calculated value of the first hyperpolarizability is 1.6567×10^{-30} e.s.u. The value of β obtained by Sun et al. [46] with the B3LYP/6-31++G(d,p) method for urea is 0.37289×10^{-30} e.s.u. The first hyperpolarizability of the title compound is 4.4 times greater than that of urea. According to the magnitude of the first hyperpolarizability, the title compound may be a potential applicant in the development of NLO materials

Table 5. Theoretical first hyperpolarizability (β) of 3'-nitroacetophenone using DFT/B3LYP/6-311++G(d,p) methods and basis set.

Parameters	Values
β_{xxx}	231.476870
β_{xxy}	7.375913718
β_{xyy}	-115.3537548
β_{yyy}	-186.703748
β_{xxz}	6.0869233
β_{yyz}	-0.1824346
β_{xzz}	-26.3916448
β_{yzz}	9.8780137
β_{zzz}	-9.5524493
first hyper polarizability	1.6567×10^{-30} e.s.u

HOMO–LOMO analysis

The energy gap between the highest occupied and the lowest unoccupied molecular orbitals, is a critical parameter in determining molecular electrical transport properties because it is a measure of electron conductivity. The analysis of the wave function indicates that the electron absorption corresponds to the transition from the ground to the first excited state and is mainly described by one-electron excitation from HOMO to LUMO. The HOMO energy characterizes the ability of electron giving and the LUMO energy characterizes the ability of electron accepting, and the gap between HOMO and LUMO characterizes the molecular chemical stability. The energy gaps are largely responsible for the chemical and spectroscopic properties of the molecules. This is also used by the frontier electron density for predicting the most reactive position in p-electron systems and also explains several types of reaction in conjugated system [47]. The HOMO and LUMO energies of 3'NAP calculated by the DFT level are listed in Table 6. The few frontier orbitals of 3'NAP are shown in Fig 5 along with the respective energies. In 3'NAP, both HOMO and LUMO are formed primarily from p_z orbital from all atoms of the compound.

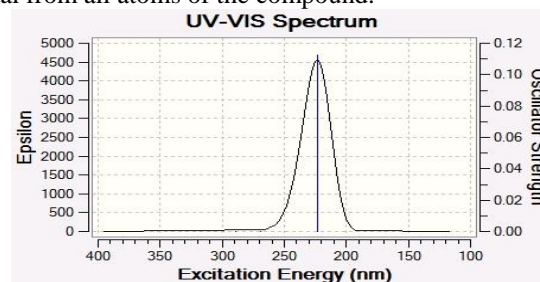


Fig 5. Single excited state absorption spectrum of 3'-nitroacetophenone.

The calculated energy value of HOMO is -0.38728 a.u. and energy of LUMO is 0.02396 a.u. Moreover lower in the HOMO and LUMO energy gap explains the eventual charge

transfer interactions taking place within the compound, which influences the biological activity of the compound and also energy serves as a measure of the excitability of a compound, the smaller the energy gap, the more easily the compound will be excited. Consequently, the lowering of the HOMO–LUMO band gap is essentially a consequence of the large stabilization of the LUMO due to the strong electron–acceptor ability of the electron–acceptor group. By using HOMO and LUMO energies, the chemical hardness (η) and chemical potential (μ) have been calculated. The chemical hardness, which is an index of reactivity, is given by

$$\eta = (I-H)/2$$

and the chemical potential that measures the escaping tendency of electron cloud is given by $\mu = -(I+H)/2$

where I and H are ionization potential and electron affinity of a molecular system. The calculated value of chemical hardness and chemical potential of 3'NAP are presented in Table 6. The usefulness of these quantities have been recently demonstrated in understanding the toxicity of various pollutants in terms of their reactivity and site selectivity [48]

Table 6. Calculated HOMO – LUMO energy of 3'-nitroacetophenone using DFT / 6-311++G(d,p) method.

Parameters	Values (a.u)
HOMO	-0.38728
LUMO	0.02396
Energy Gap	0.41124
η	0.20562
μ	0.4352

UV-VIS analysis

In the UV-VIS region with high extinction coefficient, all molecules allow strong $\pi^*\pi$ and $\sigma^*\sigma$ transition [49]. The theoretically calculated UV spectrum of 3'NAP are plotted as shown in fig 6. in an attempt to understand the nature of electronic transitions in terms of their energies and oscillator strengths, time-dependent DFT(TD-DFT) Calculations involving configuration interaction between the singly excited electronics states are conducted the calculated results involving the vertical excitations energies their molecular orbital contribution oscillator(f) and wave lengths are reported in Table 7 due to the frank Condon principle, the maximum absorption peak (max) in a uv-vis spectrum corresponds to vertical excitation. TD-DFT calculation predict three transitions in the near ultra-violet region for 3'NAP the strong transitions at 5.5484ev(223.46.nm) with an oscillator strength 0.1126 for 3'NAP.

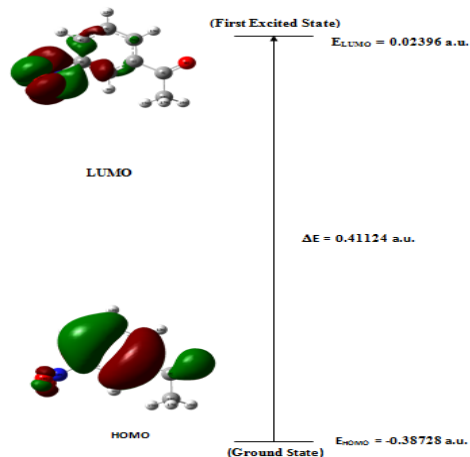


Fig 6. The few frontier orbitals of 3'-nitroacetophenone.

Table 7. The computed excitation energies, Oscillator strength and electronic transition configuration of 3'-nitroacetophenone.

Excited State	EE(eV) / Wavelength (nm)	f	Configuration	CI expansion coefficient
1	4.2812/289.60	0.0000	39→44	0.61244
			39→46	0.13223
			39→53	0.23727
2.	4.6027/269.37	0.0002	41→44	-0.12384
			41→46	0.53183
			41→50	0.13729
			41→57	0.15402
			41→59	0.14094
			41→63	0.12605
			41→64	0.17669
			41→69	-0.13073
3.	5.5487/223.46	0.1126	42→44	0.47907
			42→46	0.12494
			43→44	-0.37434
			43→46	0.24386

Error analysis of different vibrational calculations

The root mean square deviation is very small in B3LYP/6-311++G(d,p) method, B3LYP, and HF levels are shown a uniform deviation after scaling. Most of the calculated frequencies in DFT/B3LYP/6-311++G(d,p) method are exactly fitted with experimental frequencies. The correlation graphs are shown in Fig.7, which are described harmony between the calculated and experimental wavenumbers. The relations between the calculated and experimental wavenumbers are linear and described by the following equation:

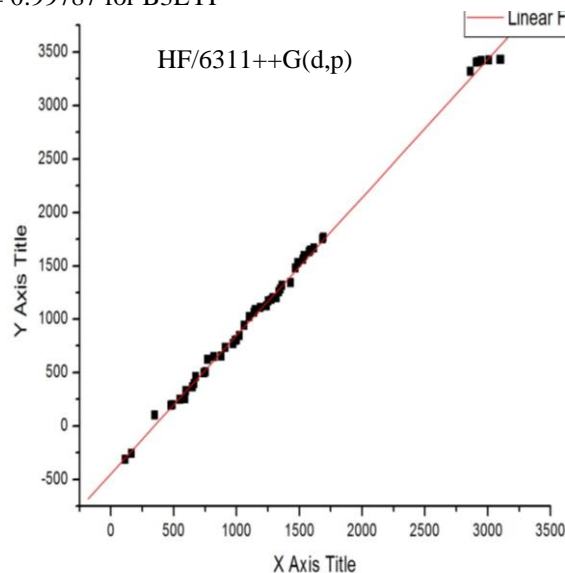
$$V_{cal} = -446.52558 V_{exp} + 1.29255 \text{ for HF=6-311++G(d,p)}$$

$$V_{cal} = -446.57049 V_{exp} + 1.2413 \text{ for B3LYP=6-311++G(d,p)}$$

We calculated correlation coefficients (R^2) value between the calculated and experimental wavenumbers. As a result, the performances of the B3LYP method with respect to the prediction of the wavenumbers within the molecule were quite close.

$$R^2 = 0.99886 \text{ for HF}$$

$$R^2 = 0.99787 \text{ for B3LYP}$$



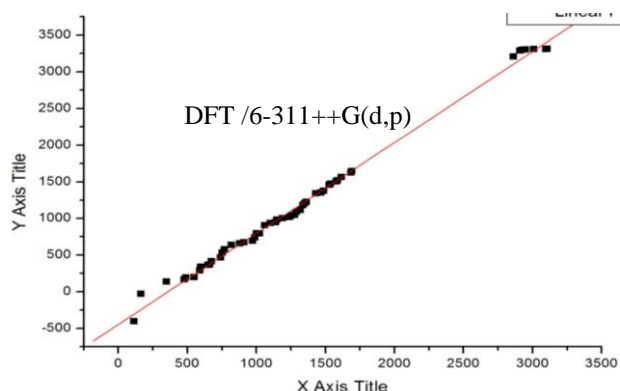


Fig 7. Correlation graph of trans 3'-nitroacetophenone . Thermodynamic Properties

Several thermodynamic parameters have been calculated using B3LYP with 6-311++G(d,p) basis set. The standard heat capacities ($C_{p,m}^0$), standard entropies (S_m^0), and standard enthalpy changes (ΔH_m^0) ($0 \rightarrow T$) were obtained and are listed in Table 8. As can be seen from in Fig 8, the standard heat capacities, entropies and enthalpy changes increase at any temperature from 100.00 to 1000.00 K, since increasing the temperature causes an increase in the intensity of the molecular vibration.

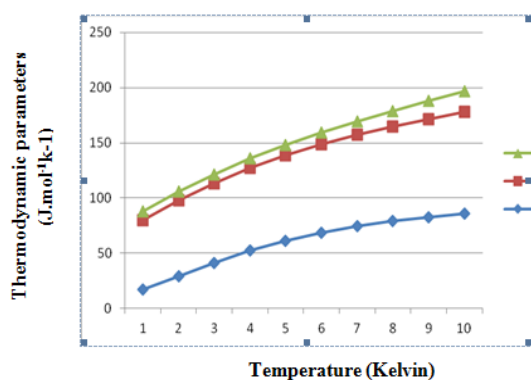


Fig 8. Correlation graph of heat capacity, entropy and enthalpy with Temperature of 3'-nitroacetophenone.

Table 8. Thermodynamic parameters of 3'-nitroacetophenone calculated using B3LYP/6-311++G(d,p) method and basis set.

(Temp)	C_p (Jmol ⁻¹ k ⁻¹)	$\Delta H_{O \rightarrow T}$ (KJ mol ⁻¹)	S (mol k ⁻¹)
100	16.9740109	7.948	63.17409
200	29.1916396	7.948004	68.68326
300	41.4370211	7.948725	71.90664
400	52.486957	8.486665	74.7311
500	61.5575183	9.274254	77.29224
600	68.7307167	10.46703	79.93412
700	74.4132581	12.04622	82.73851
800	78.9938406	13.97467	85.72827
900	82.7578519	16.2103	88.90004
1000	85.9002854	18.71273	92.23989

Conclusion

In this investigation, HF and density functional calculations on 3'-Nitroacetophenone have been performed. The main objective is to reproduce the molecular geometry, investigate the energetic behaviour (UV-VIS), reactive sites, delocalization of electron density, energy gap, and non-linear optical properties of 3'-Nitro acetophenone for the further studies. The HOMO-LUMO energy gap explain the eventual charge transfer taking place with the molecule. The molecular

electrostatic potential map shows that the negative potential sites are on the electronegative atoms as well as the positive potential sites are around the hydrogen atoms. These sites give information about the possible areas for inter- and intra molecular hydrogen bonding. Natural bond orbital analysis indicates the strong intra molecular interactions. Natural bond orbital analysis of 3'-Nitro acetophenone confirms that the intra molecular charge transfer caused by π -electron cloud movement from donor to acceptor must be responsible for the non-linear optical properties of the title compound. The correlations between the thermodynamic properties $C_{p,m}^0$, S_m^0 and H_m^0 vs temperature T are also obtained.

References

- 1.R.N. Griffin, Photochem. Photobiol. 7, 1968, 159–173.
2. L. Lindqvist, J. Phys. Chem. 76, 1972, 821–822.
3. X. Zhang, L. Shan, H. Huang, X. Yang, X. Liang, A. Xing, H. Huang, X. Liu, J. Su, W. Zhang, J. Pharm. Biomed. Anal. 49, 2009, 715–725.
4. Z.B. Liu, Y.S. Sun, J.H. Wang, H.F. Zhu, H.Y. Zhou, J.N. Hu, J. Wang, Sep. Purif. Technol. 64, 2008, 247–252.
5. Y.R. Prasad, A.S. Rao, R. Rambabu, Asian J. Chem. 21, 2009, 907–914.
6. S. Cacchi, G. Fabrizi, F. Gavazza, A. Goggiamani, Org. Lett. 5, 2003, 289–291.
7. P.M. Sivakumar, G. Sheshayan, M. Doble, Chem. Biol. Drug Des. 72, 2008, 303–313.
8. H.Z. Wei, L.C. Wing, H.L. Yuan, S.S. Yau, C.L. Yong, H.Y. Chi, Heterocycles, 45, 1997, 71–75.
9. M.J. Climent, A. Corma, S. Iborra, A. Velty, J. Catal. 221, 2004, 474–482
10. M.J. Frisch, J.A. Pople, J.S. Binkley. Journal of Chemical physics, 80(1984) 3265
11. t.clark, j.chandrasekar, g.w.spitznagel, p.v.r. schleyer journal of computational chemistry (1983)294.
12. N.sundharaganesan s.lakiamani H.Saleem. P.M. Wojciehowski, D.Michalska spectrochimica acta A61(2005)2995
13. M.J. Frisch, G.W. Trucks, H.B. Schlegel, G.E. Scuseria, M.A. Robb, J.R. Cheeseman, J.A. Montgomery, T. Vreven Jr., K.N. Kudin, J.C. Burant, J.M. Millam, S.S. Iyengar, J. Tomasi, V. Barone, B. Mennucci, M. Cossi, G. Scalmani, N. Rega, G.A. Petersson, H. Nakatsuji, M. Hada, M. Ehara, K. Toyota, R. Fukuda, J. Hasegawa, M. Ishida, T. Nakajima, Y. Honda, O. Kitao, H. Nakai, M. Klene, X. Li, J.E. Knox, H.P. Hratchian, J.B. Cross, C. Adamo, J. Jaramillo, R. Gomperts, R.E. Stratmann, O. Yazyev, A.J. Austin, R. Cammi, C. Pomelli, J.W. Ochterski, P.Y. Ayala, K. Morokuma, G.A. Voth, P. Ssalvador, J.J. Dannenberg, V.G. Zakrzewski, S. Dapprich, A.D. Daniels, M.C. Strain, O. Farkas, D.K. Malick, A.D. Rabuck, K.Raghavachari, J.B. Foresman, J.V. Ortiz, Q. Cui, A.G. Baboul, S. Clifford, J. Cioslowski, B.B. Stefanov, G. Liu, A. Liashenko, P. Piskorz, I. Komaromi, R.L. Martin, D.J. Fox, T. Keith, M.A. Al-Laham, C.Y. Peng, A. Nanayakkara, M. Challacombe, P.M.W. Gill, B. Johnson, W. Chen, M.W. Wong, C. Gonzalez, J.A. Pople, Gaussian Inc., Pittsburgh PA, 2009]
14. T. Sundius, Journal of molecular structure. 218 (1990) 321.
15. MOLVIB (V.7.0): calculation of Harmonic force field and vibrational modes of molecules. QCPE program No.807 (2002).
16. T. Sundius vibrational spectroscopy 29(2002) 89.
17. G. Keresztury, S. Holly, J. Varga, G. Besenyey, A.Y. Wang, J.R. Durig, Spectrochim. Acta Part A, 49 (1993) 2007

18. P.L. Polavarapu, *J. Phys. Chem.*, 94 (1990) 8106
19. R.M. Silverstein, G. Clayton Bassler, Morrill, *Spectrometric identification of Organic Compounds*, John Wiley and Sons, New York, 1991
20. N. Sundaraganesan, S. Kalaichelvan, C. Meganathan, B. Dominic Joshua, J. Cornard, *Spectrochim Acta*, 71A (2008) 898.
21. M. Haisa, T. Setsuokashino, K.A. Yuasa, *Acta Crystallogr*, 32B (1976) 1326.
22. C.P. D Dwivedi, S.N. Sharma, *Indian J. pure and applied physics* 11 (1973) 447.
23. K.M. Gough. B.R. Herry, *J. Phy. chem.* 87 (1983) 3804.
24. D. Mahadevan S. Periandy, M. Karaback, S. Ramalinagam, N. Puviarasan, *Spectrochim Acta*, A86 (2012) 139.
25. M. Arivazhagan S. Manivel S. Jeyavijayan R. Meenakshi *Spectrochimica Acta Part A: Molecular and Biomolecular Spectroscopy* 134 (2015) 493–501
26. M. Arivazhagan R. Kavitha, V.P. Subhasini, *Spectrochim Acta part A: molecular and Bio molecular spectroscopy* 130 (2014) 502-515.
27. M. Arivazhagan, S. Jeyavijayan, *Spectrochimica Acta Part A* 79 (2011) 161–168.
28. S. jeyavijayan *Indian Journal of pure & Applied Physics* vol.53.March 2015,pp.151-159
29. M. Elanthiraiyan B. Jayasudha, and M. Arivazhagan *Elixir Vib. Spec.* 86 (2015) 35018-35027
30. R.M. Silverstein, G. Clayton Bassler, T.C. Morrill, *Spectroscopic Identification of Organic Compounds*, John Wiley, New York, 1991.
31. B.S. Furnell, *Vogel Text Book of Practical Organic Chemistry*, 5th edition, Long ManWidely, New York, 1989.
32. N. Sundaraganesan, B. Dominic Joshua, *Spectrochimica Acta*, Part A 68 (2007) 771– 777.
33. S. Mohan, N. Sundaraganesan, J. Mink, *Spectrochimica Acta A* 47 (1991) 1111.
34. V. Krishnakumar, N. Prabavathi, *Spectrochimica Acta*, Part A 72 (2009) 743– 747.
35. N. Sundaraganesan, S. Ayyappan, H. Umanaheswari, B. Dominic Joshua, *Spectrochim. Acta* 66A (2007) 17-27.
36. M. Arivazhagan, R. Kavitha *Jouranal of molecular structure* 1011 (2012) 111-120.
37. A.E. Reed, L.A. Curtiss, F. Wenhold, *Chem. Rev.* 88 (1988) 899–926.
38. E.D. Glendening, J.K. Badenhoop, A.E. Reed, J.E. Carpenter, J.A. Bohmann, C.M. Morales, F. Weinhold, *NBO 5.0*, third ed., Theoretical Chemistry Institute, University of Wisconsin, Madison, 2001.
39. F. Weinhold, *Nature* 411 (2001) 539–541.
40. F. Weinhold, C. Landis, *Valence and Bonding: A Natural Bond Orbital Donor- Acceptor Perspective*, Cambridge University Press, Cambridge, 2005
41. D.Sajan, J.Hubert, V.S. Jayakumar. J.Zaleski. *J.Mol. Struct.* 785 (2006)43.
42. C.E.Powel.M.G.Humphrey, *coord. chem..rev.*24 (2004)725
43. K.S.Thanthiriwatte K.M.Nalin de Silva.J. Mol. Struct. (Theochem) 617(2002)169
44. L.Fang.G.C.Yang, Y.Q.Qiu.Z.M.Su.Theo.Chem.Acc.119(2008)329
45. Y.X.Sun, Q L.Hao.W.X.Wei, .Z.X. YU. L.D. LVX. Wang, Y.S. Wang.*j.mol.struct,(Theochem)*904 (2009)74.
46. W.J.Chi, L.LI. B.-T..Li,H-S.Wu,*J.Mol.Modal* 2012, DOI: 101007/s00894-012-1359-6
47. K. Fukui, T. Yonezawa, H. Shingu, *J. Chem. Phys.* 20 (1952) 722.
48. R. Parthasarathi, J. Padmanabhan, V. Subramanian, B. Maiti, P.K. Chattraj, *Curr. Sci.* 86 (2004) 535–542
49. P.W.Atkins,*physical chemistry*, Oxford university press, Oxford, 2001.